Nuclear Instruments and Methods in Physics Research A 845 (2017) 452–458

Contents lists available at ScienceDirect

Nuclear Instruments and Methods in Physics Research A

journal homepage: www.elsevier.com/locate/nima

Test-beam and laboratory characterisation of the TORCH prototype detector

A. Ros [a,*], N.H. Brook [b], L. Castillo-Garcia [d], T. Conneely [e], D. Cussans [a], K. Foehl [d], R. Forty [d], C. Frei [d], R. Gao [c], T. Gys [d], N. Harnew [c], J. Milnes [e], D. Piedigrossi [d], J. Rademacker [a], M. Van Dijk [a]

[a] University of Bristol, H.H. Wills Physics Laboratory, Bristol BS8 1TL, UK
[b] University College London, Department of Physics & Astronomy, Gower Street, London WC1E 6BT, UK
[c] University of Oxford, Denys Wilkinson Building, 1 Keble Road, Oxford OX1 3RH, UK
[d] CERN, EP Department, CH-1211 Geneva 23, Switzerland
[e] Photek Ltd, St. Leonards-on-Sea TN38 9NS, UK

ARTICLE INFO

Article history:
Received 24 March 2016
Received in revised form
7 June 2016
Accepted 15 June 2016
Available online 16 June 2016

Keywords:
Cherenkov radiation
Particle identification
TORCH
MCP-PMT

ABSTRACT

The TORCH time-of-flight (TOF) detector is being developed to provide particle identification up to a momentum of 10 GeV/c over a flight distance of 10 m. It has a DIRC-like construction with 10 mm thick synthetic amorphous fused-silica plates as a Cherenkov radiator. Photons propagate by total internal reflection to the plate periphery where they are focused onto an array of customised position-sensitive micro-channel plate (MCP) detectors. The goal is to achieve a 15 ps time-of-flight resolution per incident particle by combining arrival times from multiple photons. The MCPs have pixels of effective size 0.4 mm × 6.6 mm^2 in the vertical and horizontal directions, respectively, by incorporating a novel charge-sharing technique to improve the spatial resolution to better than the pitch of the readout anodes. Prototype photon detectors and readout electronics have been tested and calibrated in the laboratory. Preliminary results from testbeam measurements of a prototype TORCH detector are also presented.

1. Introduction

The goal of the TORCH (Timing Of internally Reflected CHerenkov photons) detector is to achieve a 15 ps time-of-flight resolution per incident charged particle over a flight distance of 10 m. TORCH is designed for large-area coverage, of approximately 30 m^2, and has been proposed for the upgrade of the LHCb experiment to complement the particle identification capabilities of the RICH detectors. The timing precision is accomplished by combining arrival times from multiple photons, requiring a resolution of 70 ps for single photons [1]. A schematic of a single module of the TORCH detector is shown in Fig. 1.

A prototype TORCH detector has been constructed which is a scaled-down version of the full TORCH module, and consists of a synthetic amorphous fused-silica bar, 120 × 350 × 10 mm^3 (width × length × thickness), coupled to a quartz block with a mirrored cylindrical surface that focusses the Cherenkov photons onto position-sensitive microchannel plate photomultiplier (MCP-PMT) detectors. A customised MCP, shown in Fig. 2, has been developed in industrial partnership with Photek, UK. This so-called Phase-2 MCP has a circular 40 mm diameter housing and 26.5 × 26.5 mm^2 active area.

The spatial resolution required by TORCH is $0.4\,\text{mm}/\sqrt{12} = 0.12$ mm in the "fine" (vertical) direction. The MCP-PMT has 0.8 mm^2 square pixels. A novel method of coupling the MCP-PMT output pads to an interface-PCB through an Anisotropic Conductive Film (ACF) is used, together with customised readout electronics. The back-plane anode is formed by metallic pads connected to the PCB that merges channels in groups of 8 in the "coarse" (horizontal) direction, resulting in an array of 4 × 32 logical pixels for the Phase-2 MCP-PMT. The aim is to produce square 2 × 2 in.^{2} long-lifetime MCP-PMT detectors with 8 × 64 logical pixels for the final stage (Phase-3) of TORCH development. Charge sharing between pixels maintains the required spatial resolution whilst halving the number of readout channels.

Fig. 3 is an example of a hit-map pattern that would be expected in the TORCH prototype, produced using a GEANT4 simulation with 180 GeV/c protons traversing the centre of the TORCH module [2]. Cherenkov light is internally reflected in the quartz bar and is detected on the plane of MCP-PMTs via an additional

* Corresponding author.
E-mail address: ana.rosgarcia@bristol.ac.uk (A. Ros).

http://dx.doi.org/10.1016/j.nima.2016.06.087

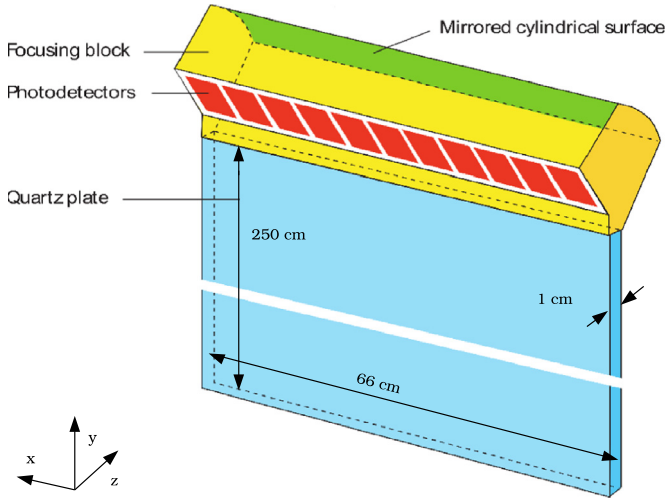

Fig. 1. A module of the TORCH detector ($66 \times 250 \times 1$ cm^3). The TORCH modular consists of 18 such modules with a overall area of about 6×5 m^2.

reflection in the focussing block. A folding of the image pattern is observed due to reflections from the side faces of the quartz bar; there is also a finite width of the pattern resulting from chromatic dispersion in the quartz. It is important to correctly distinguish photons that have one or more side reflections from those that do not, because these class of reflections correspond to different path lengths, and hence times of propogation, of the photons inside the quartz bar.

2. Readout chain characterisation

The readout chain for the TORCH prototype detector is based on the NINO front-end amplifier/discriminator ASIC that was originally developed for the TOF system of ALICE, along with the HPTDC chip for digitisation [3,4]. Customised electronics boards have been developed using a 32-channel version of the NINO chip and HPTDC, as shown in Fig. 4.

The performance of the MCP and full electronics readout chain has been studied with a Picosecond Diode Laser system (PiLas-Advanced Laser Diode Systems) attenuated to produce single photons, and optimised for measurements of efficiency, spatial and time resolution. Laboratory measurements of the charge to width calibration of the NINO32 were made using a pulse generator to inject charge and an oscilloscope to record the output signals. The calibrations over several channels, with a programmed threshold of 60 mV for the Time Over Threshold (TOT) NINO front-end amplifier/discriminator, are shown in Fig. 5. The curves exhibit two important features. Firstly the calibration of charge-to-width is not linear, and secondly the behaviour changes from channel-to-channel and from chip-to-chip. This demonstrates that it is necessary to perform a charge-to-width calibration on every individual channel.

The Phase-2 MCP-PMT tube was tested in the laboratory to understand its charge-sharing properties. The measurements were performed with the laser scanning over four pixels of the tube in 0.414 mm steps (half the width of a pixel). The hit position was then calculated using a Centre of Gravity (CoG) algorithm in which the CoG was first calculated from the position of the pixel centroids weighted by the uncalibrated TOT widths of the signals $P_w = \sum_i w_i x_i / \sum_i w_i$, where the sum is overall pixels. Fig. 6 shows the actual laser position on the MCP-PMT photocathode as a function of the resulting measured position. The estimated position was then re-calculated by using the CoG weighted with the charges calculated from the charge-to-width calibration curves: $P_q = \sum_i q_i x_i / \sum_i q_i$. The resulting linear behaviour, also seen in Fig. 6, illustrates that the charge sharing method is effective in achieving improved spatial accuracy, however it also reinforces the importance of accurate NINO calibrations.

Previous measurements of the NINO readout demonstrate that a spatial resolution of $\sigma = 0.031$ mm is achievable [5]. These measurements were performed with a different MCP-PMT, readout electronics and calibration methodology to that presented here. Futher studies with different tubes and readout

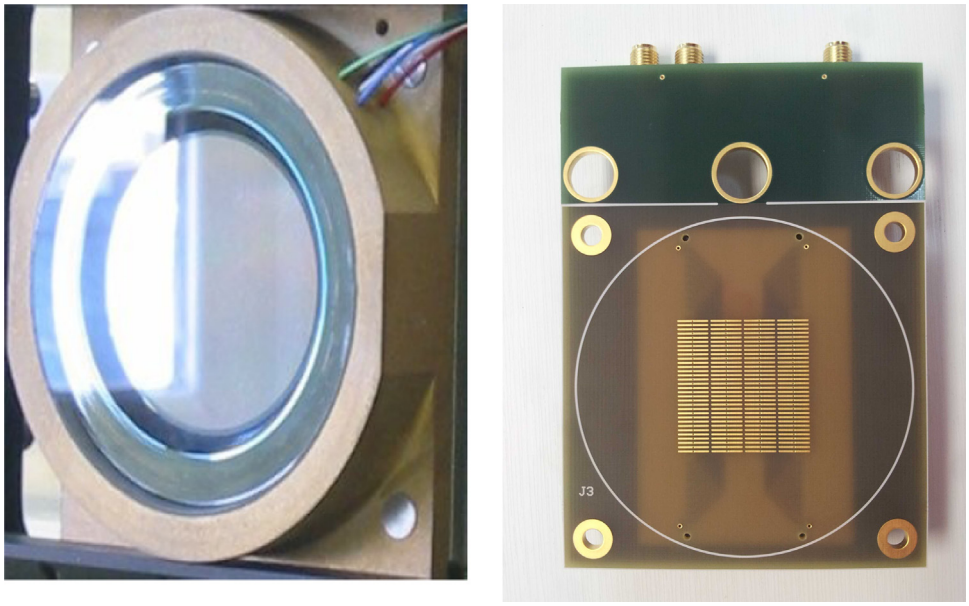

Fig. 2. (Left) View through the entrance window of the Phase-2 Photek MCP-PMT, which has an active area of 26.5×26.5 mm^2; (Right) The backplane of the MCP-PMT.

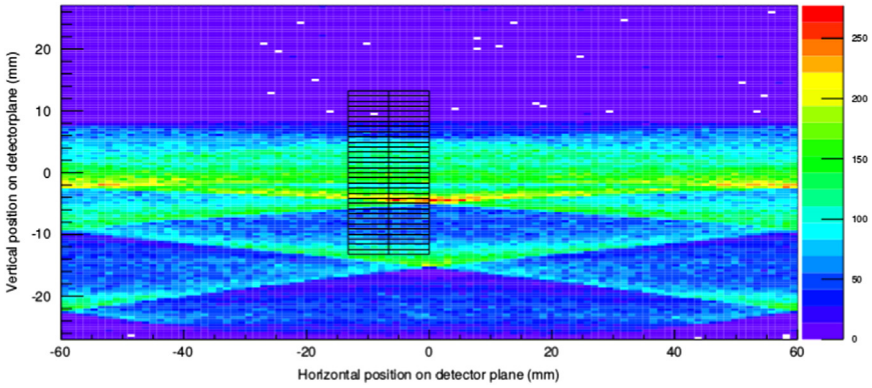

Fig. 3. A hit-map pattern expected from a fully instrumented TORCH prototype module. The area outlined in black shows the expected hit-map pattern measured by a single Phase-2 MCP-PMT.

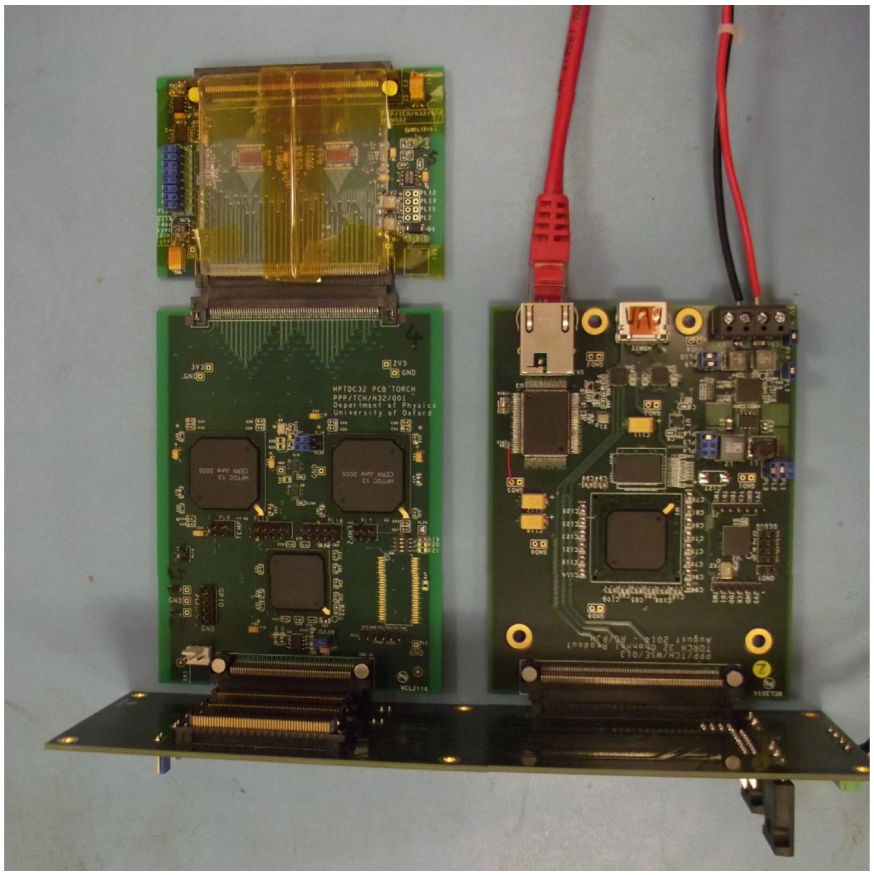

Fig. 4. A photograph of the customised electronic boards for TORCH. The NINO board is at the top left side, the HPTDC board on the bottom left side. The readout board on the right is connected through an Ethernet cable to the control PC. The HPTDC and readout boards are connected through a back-board that has the capability to operate with four NINO and HPTDC boards.

boards will be undertaken to study the optimal spatial resolution performance.

3. Testbeam preliminary results

Studies of the TORCH prototype detector, shown in Fig. 7, have been performed at the CERN PS testbeam facility using a π/p beam of 1–12 GeV/c momentum; the nominal beam composition was 67% pions and 33% protons at 3 GeV/c. The purpose of the tests was to understand the spatial and timing resolutions of TORCH in a realistic environment and to optimise the TORCH design. The PS facility provides two Cherenkov threshold counters and one scintillation detector. The TORCH MCP-PMT, readout electronics and radiator with focussing quartz block were housed in a light-tight box. A pair of scintillation finger modules, each containing one plastic scintillator read out by a PMT, provided an event trigger. In each of these two modules, a borosilicate bar acting as a source of prompt Cherenkov light and read out by a single channel MCP, provided a start/stop timing reference. The stations, shown in

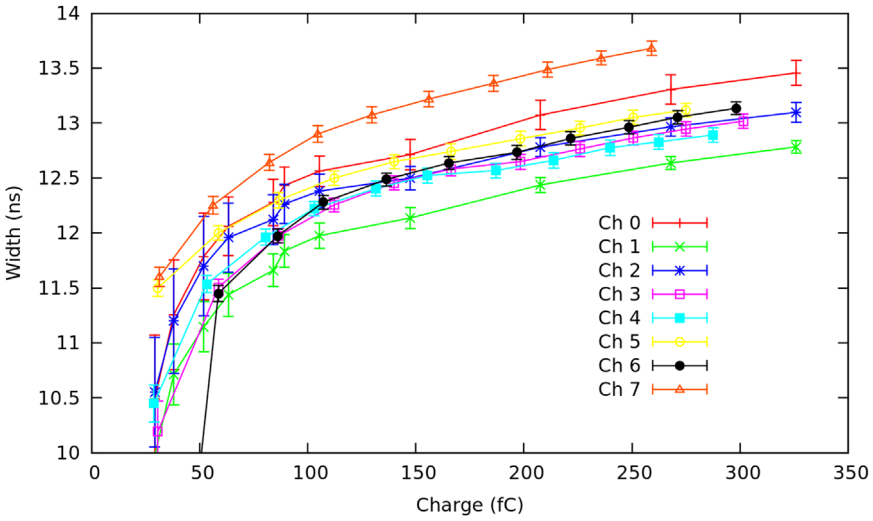

Fig. 5. Charge-to-width calibration for eight NINO32 channels with a threshold setting of 60 mV.

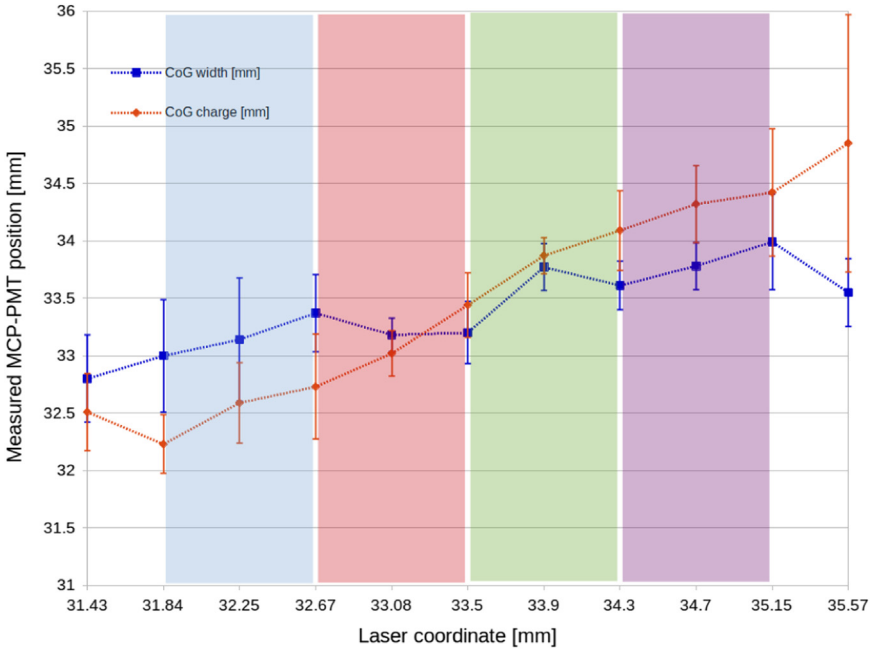

Fig. 6. A laser scan of the Phase-2 MCP, showing the known laser position as a function of the measured MCP-MCP coordinate. The blue points show the position calculated using the CoG method with the average pixel positions weighted by the measured widths of the signals P_w, and the orange points show the position calculated using the average pixel positions weighted with calibrated charges P_q. The four coloured areas in the plot refer to the four pixels of the tubes over which the scan was performed. The errors-bars are the 68% confidence intervals of the fitted distributions from each of the measurement points. (For interpretation of the references to colour in this figure legend, the reader is referred to the web version of this article.)

Fig. 7, were separated by a distance of 10.60 m. The reference time measurements were made by either commercial electronics or the TORCH readout system.

Reference measurements of the time of flight of 3 GeV/c beam particles between the two borosilicate stations were made in order to compare the timing resolution of the TORCH readout electronics (with an HPTDC time binning of 100 ps) and with the commercial module (with a time binning of 6.25 ps). Figs. 8 (Top and Bottom) compare the reference TOF distributions for protons and pions measured with the commercial module and with the TORCH readout, respectively. The TOF difference is found to be $\Delta t \approx 1638 \pm 5$ ps for the commercial setup and $\Delta t \approx 1680 \pm 11$ ps for the TORCH readout. Any discrepancy can be attributed to systematic differences in the time binning of the two systems. These results agree with the expected time of flight difference between pions and protons of $\Delta t \approx 1690$ ps at 3 GeV/c over the nominal flight path.

Preliminary results from the TORCH prototype are compared with simulation in Fig. 9. The simulations show the distribution of photon arrival times in bins of 100 ps as a function of photon position at the MCP-PMT plane. The timing of the photons and their positions form bands, corresponding to those photons

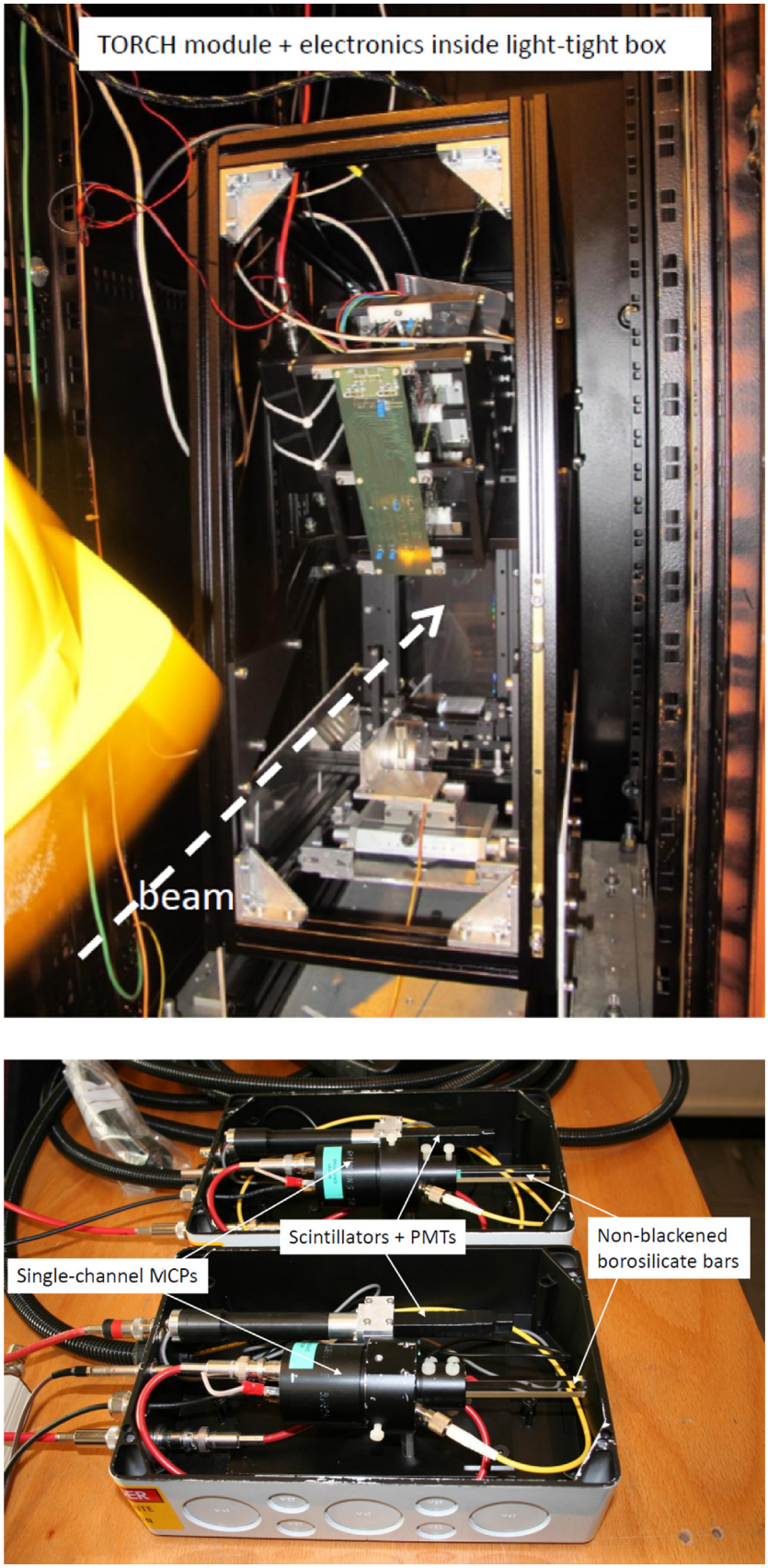

Fig. 7. (Top) The TORCH prototype module comprising a radiator plate of $120 \times 350 \times 10\ \mathrm{mm}^3$, a focussing block, a Phase-2 MCP-PMT, and customised electronic boards. (Bottom) The scintillation finger modules and borosilicate bars with single-MCPs to provide a trigger and timing reference, respectively.

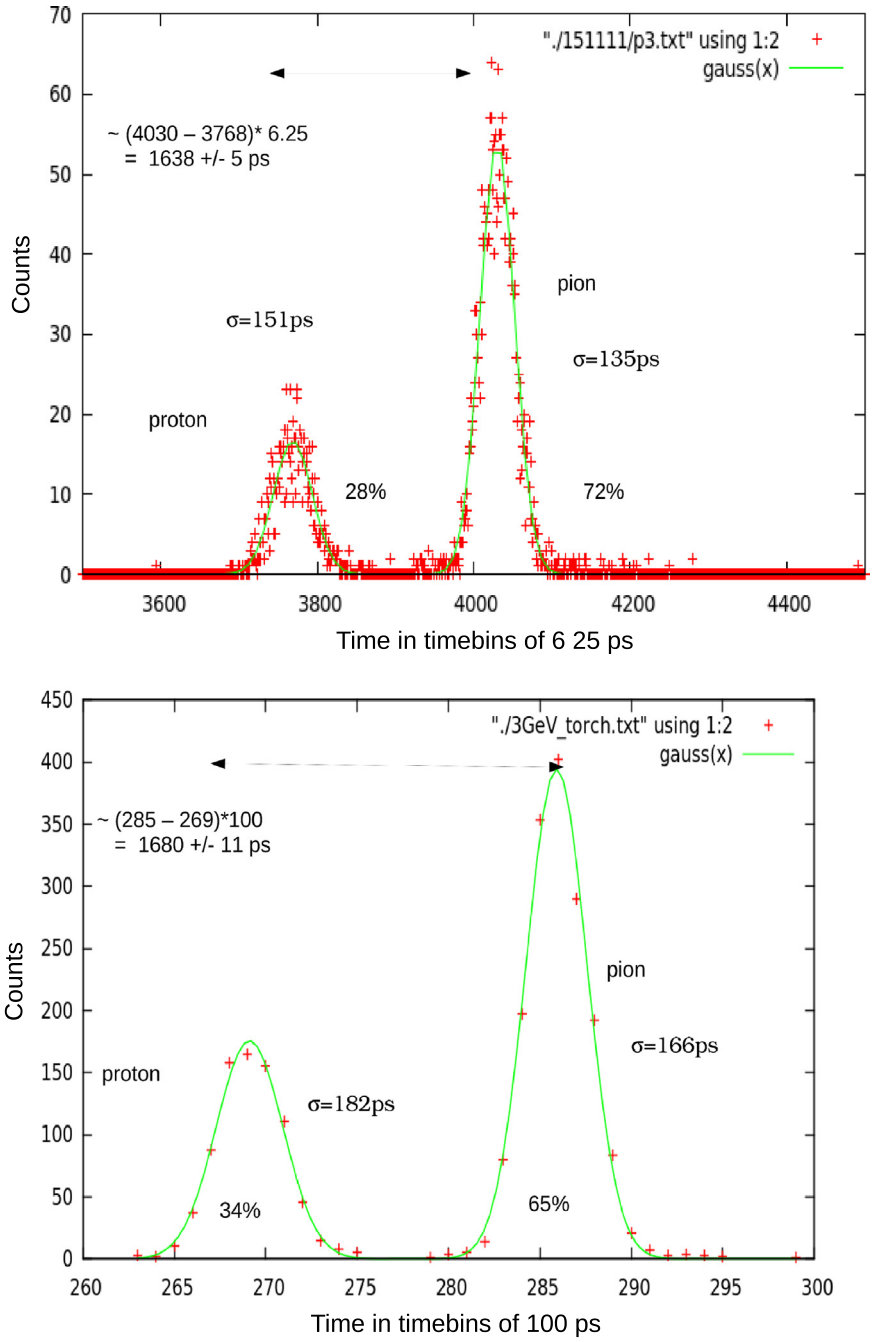

Fig. 8. (Top) The reference TOF difference of 3 GeV/c pions and protons measured over a 10.60 m flight path using commercial electronics with a 6.25 ps time binning; (Bottom) the reference TOF difference using TORCH electronics with 100 ps time binning.

arriving directly to the MCP-PMT and those with one or two reflections from the lateral sides of the quartz radiator plate. In comparison, the testbeam measurements are also shown in Fig. 9. The time projections as a function of hit pixels recorded by the fully instrumented MCP-PMT demonstrate that patterns from direct detection and from one or more side reflections can be resolved. Detailed analysis of these data is on-going.

4. Conclusions and perspectives

Prototype micro-channel plate photon detectors and readout electronics for the TORCH time-of-flight detector have been tested and calibrated in the laboratory. These detectors use charge division to provide spatial measurements that have a resolution better than the pixel width. Measurements in the laboratory with a laser scanned over the MCP photocathode show a spatial response which is linear, and giving an acceptable resolution. The measurements show the importance of a full charge to width calibration of the NINO32 electronics boards.

The first CERN-PS testbeam measurements from a prototype TORCH detector have also been presented. Preliminary results show that direct, first and double reflections from the quartz sides are distinguished in raw data. Full calibrations must now be applied to the measured data in order to achieve optimal spatial and timing resolutions.

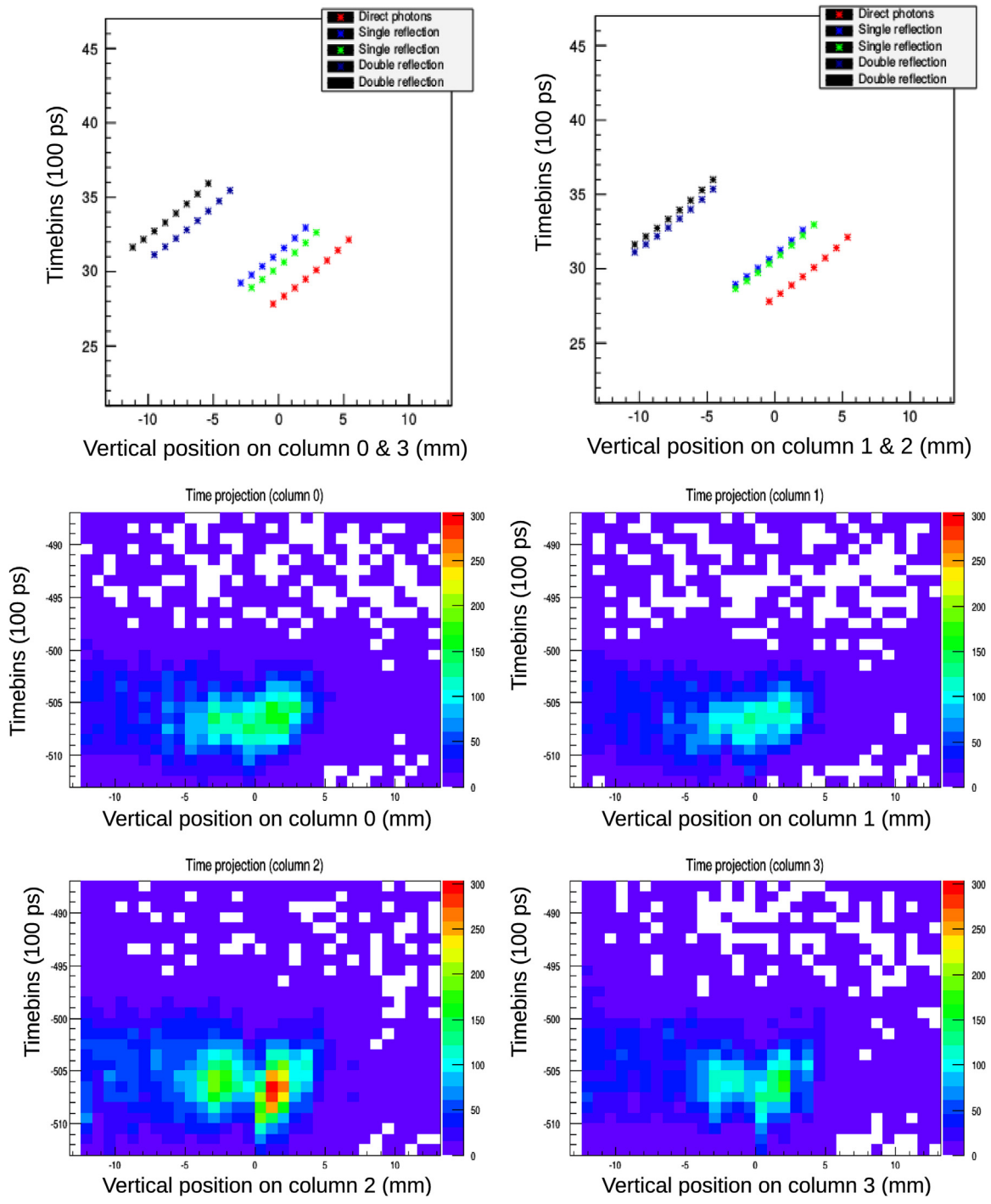

Fig. 9. (Top plots) Simulated photon arrival-time patterns as a function of MCP column number for direct light (red), one reflection (blue, green) and two reflections (dark blue, black). (Bottom and middle plots) The measured photon arrival time distributions in 100 ps bins as a function of hit position in a column (pixel number) from testbeam data. (For interpretation of the references to colour in this figure legend, the reader is referred to the web version of this article.)

Acknowledgements

The support of the European Research Council is gratefully acknowledged in the funding of this work (ERC-2011-AdG, 291175-TORCH).

References

[1] M.J. Charles, R. Forty, TORCH time of flight identification with cherenkov radiation, Nucl. Instrum. Methods A 639 (1) (2011) 173–176, http://dx.doi.org/10.1016/j.nima.2010.09.021.

[2] M.V. Dijk, Design of the TORCH detector: a cherenkov based time-of-flight system for particle identification, PhD thesis - University of Bristol.

[3] F. Anghinolfi, NINO: an ultra-fast and low-power front-end am-plifier/discriminator ASIC designed for the multigap resistive plate chamber, Nucl. Instrum. Methods A 533 (1–2) (2004) 183–187, http://dx.doi.org/10.1016/j.nima.2004.07.024.

[4] A. Akindinov, Design aspects and prototype test of a very precise TDC system implemented for the multigap RPC of the ALICE-TOF, Nucl. Instrum. Methods A 533 (1–2) (2004) 178–182, http://dx.doi.org/10.1016/j.nima.2004.07.023.

[5] L. Castillo-Garcia, Development, characterization and beam tests of a small-scale torch prototype module, DIRC2015, Workshop on Fast Cherenkov detectors. To be published in Journal of Instrumentation.